Covalent Organic Frameworks with Chirality Enriched by Biomolecules for Efficient Chiral Separation
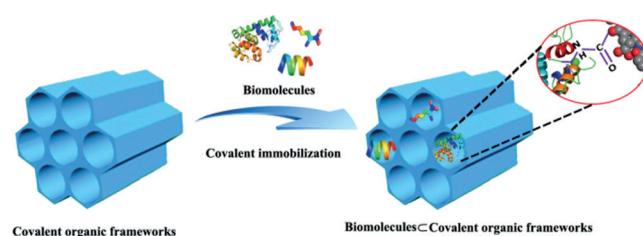
Sainan Zhang, Yunlong Zheng, Hongde An, Briana Aguila, Cheng-Xiong Yang, Yueyue Dong, Wei Xie, Peng Cheng, Zhenjie Zhang,* Yao Chen,* and Shengqian Ma*

Abstract: *The separation of racemic compounds is important in many fields, such as pharmacology and biology. Taking advantage of the intrinsically strong chiral environment and specific interactions featured by biomolecules, here we contribute a general strategy is developed to enrich chirality into covalent organic frameworks (COFs) by covalently immobilizing a series of biomolecules (amino acids, peptides, enzymes) into achiral COFs. Inheriting the strong chirality and specific interactions from the immobilized biomolecules, the afforded biomolecules⊂COFs serve as versatile and highly efficient chiral stationary phases towards various racemates in both normal and reverse phase of high-performance liquid chromatography (HPLC). The different interactions between enzyme secondary structure and racemates were revealed by surface-enhanced Raman scattering studies, accounting for the observed chiral separation capacity of enzymes⊂COFs.*

Chiral resolution is an important tool in the production of pharmaceutical and biologically active compounds, as the biological behavior, metabolism, and toxicity of pure enantiomers are often quite different.[1] The separation of racemic compounds has long been of great significance, especially for pharmaceutical and medicinal applications,[2,3] which has spurred continuous interest in the exploration of new materials/approaches for efficient separation of enantiomers.[4–7] To achieve efficient separation of enantiomers, it is essential the material possess both strong chiral environment and preferable binding ability through some specific interactions (for example, hydrogen bonding, van der Waals interactions, and electrostatic interactions).[8–10] Biomolecules such as enzymes that are created by nature,[11] can well

discriminate enantiomers owing to their natural conformations composed of chiral subunits (that is, amino acids) as well as amphiphilic and zwitterionic features capable of providing specific interactions. This makes them appealing for chiral separation particularly as chiral stationary phases (CSPs) in chromatography if they can be immobilized on some solid-state materials. Herein, we contribute a general approach to immobilize biomolecules into a new class of solid-state materials, covalent organic frameworks (COFs), and the afforded biomolecules⊂COFs can serve as versatile and highly efficient CSPs towards various racemates in both normal-phase and reverse-phase high-performance liquid chromatography.

Emerging as a new class of crystalline solid-state materials, COFs feature high surface area, low mass density, tunable pore size, high stability, and easily tailored functionality,[12–14] which means they hold promise for applications in many fields such as gas storage,[15] photoelectricity,[16] catalysis,[17–19] environmental remediation,[20] drug delivery,[21] and functional devices.[22] The development of COFs for chiral separation is still in the infancy stage,[23–25] primarily relying on the construction of chiral COFs based on chiral monomers. On the basis of our recent success in immobilizing enzymes into COFs,[26] in this work we present an alternative strategy to introduce chirality into COFs by covalently anchoring a series of biomolecules, such as amino acids, peptides, and enzymes, onto the channel walls of achiral COFs to form biomolecules⊂COFs (Scheme 1).[27–29] We postulate that inheriting the

[*] S. Zhang, Y. Zheng, H. An, Prof. Z. Zhang, Prof. Y. Chen
State Key Laboratory of Medicinal Chemical Biology
Nankai University, Tianjin 300071 (China)
E-mail: zhangzhenjie@nankai.edu.cn
chenyao@nankai.edu.cn

B. Aguila, Prof. S. Ma
Department of Chemistry, University of South Florida
4202 E. Fowler Avenue, Tampa, FL 33620 (USA)
E-mail: sqma@usf.edu

S. Zhang, Y. Zheng, H. An, Prof. Y. Chen
College of Pharmacy, Nankai University
Tianjin 300071 (China)

Prof. C.-X. Yang, Y. Dong, Prof. W. Xie, Prof. P. Cheng, Prof. Z. Zhang
College of Chemistry, Nankai University
Tianjin 300071 (China)

Supporting information and the ORCID identification number(s) for the author(s) of this article can be found under:
https://doi.org/10.1002/anie.201810571.

Scheme 1. Covalently immobilizing biomolecules into COFs.

strong chirality and specific interactions from the anchored biomolecules, the resultant biomolecules⊂COFs are anticipated to demonstrate high efficiency for chiral separation; in addition, the protective environments provided by COFs[26] and the strong covalent bonding between the biomolecules and COF channel walls thus to prevent the denaturing and leaching of biomolecules make biomolecules⊂COFs ideal chiral stationary phases in both normal-phase and reverse-phase HPLC.

To demonstrate the generality of our strategy as well as to investigate the effect of structural complexity of biomolecules on the chiral separation performance, enzymes, peptides, and amino acids were covalently anchored on the channel walls of COFs to form biomolecules⊂COFs. Lysozyme is a good candidate protein for chiral recognition and separation owing to its low cost, high thermal stability, relatively small size $(3.0 \times 3.0 \times 4.5$ nm), and facile modification.[30] To compare with lysozyme, we also used tripeptide Lys-Val-Phe (similar arrangement with NH$_2$-terminal of lysozyme) and L-lysine (abundance in lysozyme) as controls.

A new mesoporous COF **1** was designed and synthesized via a condensation reaction to immobilize biomolecules (Figure 1 a; Supporting Information, Figure S1). The powder

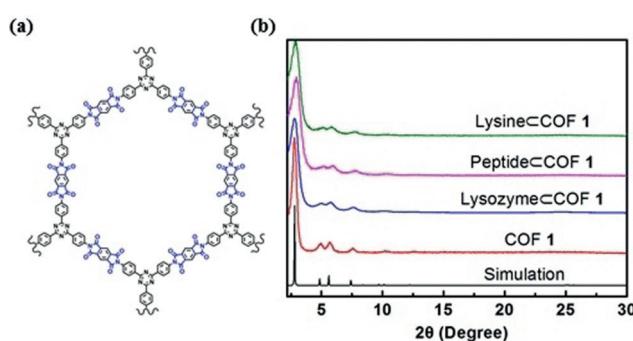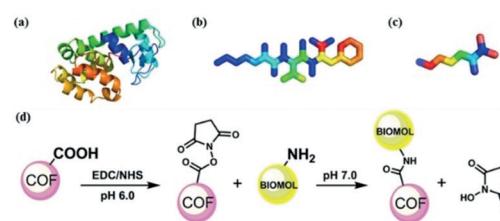***Figure 1.*** a) COF **1**. b) PXRD patterns of COF **1**, biomolecule⊂COF **1**, and the simulated pattern of COF **1**.

X-ray diffraction (PXRD) pattern of COF **1** agrees with the simulated structure with AA layer packing (Figure 1 b). The characteristic FTIR peaks at 1778 cm^{-1} and 1721 cm^{-1} can be attributed to the asymmetric and symmetric vibrations of C=O groups of the imide rings of COF **1**. The peak at about 1352 cm^{-1} revealed the successful formation of imidized networks (Supporting Information, Figure S2).[31] More specific structural information of COF **1** was confirmed by ^{13}C CP/MAS NMR spectra (Supporting Information, Figure S3). COF **1** showed a broad resonance signal overlapping from 127.8 ppm to 141.4 ppm, which corresponds to the phenyl carbon atoms. The peak at 157.7 ppm was assigned to the carbonyl carbon of the imide rings. COF **1** possesses 1D hexagonal channels with a pore size of about 3.6 nm after subtracting van der Waals radius (measured between two nitrogen atoms along the diagonal), which is large enough to accommodate biomolecules such as lysozyme. The N atoms in triazine and O atoms in imide groups are potential hydrogen bonding acceptors to interact with biomolecules. Moreover, COF **1** not only demonstrated extraordinary stability in various organic solvents (Supporting Information, Figure S4), but also exhibited excellent water stability (for example, pH 6.0 MES buffer or hot water; Supporting Information, Figure S5), which is critical for bio-related applications. The structural features together with the high water stability make COF **1** a promising platform to accommodate biomolecules.

The condensation reaction of an anhydride and a primary amine possesses a two-step mechanism (Supporting Information, Scheme S1).[32] First, the anhydride can react with the

primary amine to form amic acid intermediates via a spontaneous ring opening process. Second, while the synthesis temperature rises to $>150\,°C$, this amic acid group can dehydrate to form an imide group. Carboxylate groups ($-$COOH) can exist as residuals during this condensation reaction. To determine the amount of accessible $-$COOH residues, analysis methods including Toluidine blue O (TBO) dye assay and acid–base titration method were employed.[33–35] The results revealed synthesis temperature and ratio of reactants played critical roles to the amount of accessible $-$COOH in COF **1** (Supporting Information, Figure S6). Finally, we employed COF **1** that was synthesized at 200 °C using reactants of stoichiometric mole ratio as the major focus of further study because it exhibited the best crystallinity (Supporting Information, Figure S7) as well as a good amount of $-$COOH residues (5.1% and 5.7% determined by TBO assay and acid–base titration, respectively). The accessible $-$COOH is potential to react with $-$NH$_2$ residues in biomolecules, which make COF **1** a perfect platform to immobilize biomolecules via covalent bonding.

To efficiently enrich chirality into COFs using biomolecules, we employed a covalent coupling strategy (Scheme 2) to immobilize biomolecules via a coupling reaction of $-$NH$_2$

Scheme 2. Views of tested biomolecules: a) lysozyme, b) tripeptide Lys-Val-Phe, c) lysine. d) Illustration of the covalent strategy to bond various biomolecules with COFs.

(from the biomolecules) and $-$COOH (from the COFs) using 1-ethyl-3-(3-dimethylaminopropyl) carbodiimide (EDC) and N-hydroxysuccinimide (NHS). This reaction is widely applied for immobilization of biomolecules.[36,37] We first compared this strategy with traditional adsorption methods. Lysozyme, tripeptide Lys-Val-Phe, and L-lysine (Scheme 2) were loaded by adsorption in COF **1** to form biomolecules@COF **1** (@ here means adsorbed in) in comparison with covalently bonded biomolecules⊂COF **1** (⊂ here means covalently bonded with). The loading amount of lysozyme with the covalent immobilization method (Figure 2 a, ca. 22 μmol g^{-1}) was almost double that with the adsorption method (ca. 12 μmol g^{-1}). Inversely, the leakage of lysozyme for the covalent method was far lower than that for the adsorption method (Figure 2 b). In the covalently loaded systems, we observed nearly no leaching of lysozyme from lysozyme⊂COF **1**. However, in the adsorption systems, the leakage of lysozyme came up to about 90% from Lysozyme@COF **1**. Similarly, the loading amounts of peptide and L-lysine with the covalent method were much higher than the amount with adsorption method (Supporting Information, Figure S8). The leakages of peptide and L-lysine that were covalently
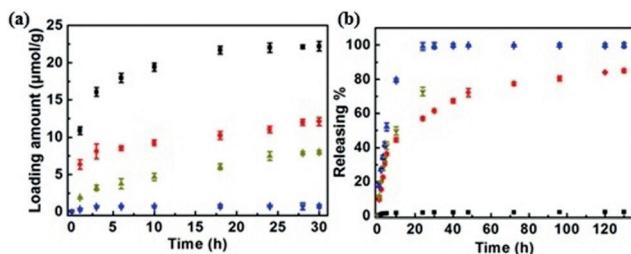
Figure 2. a) Loading profiles and b) releasing profiles of lysozyme into and form COF **1** and other tested porous supports. Lysozyme⊂COF **1** (black), lysozyme@COF **1** (red), lysozyme@PCN-600 (dark yellow), lysozyme@MCM-41 (blue).

immobilized in COF **1** were as low as 6% and 7%, which were far lower than the adsorption systems (ca. 90% and ca. 91% leaching for Peptide@COF **1** and Lysine@COF **1**, respectively; Supporting Information, Figure S8). These results reveal that there are strong binding interactions between biomolecules and COF **1** in biomolecule⊂COF **1** systems. In contrast, in biomolecule@COF **1** systems, the absence of a strong interaction between the host matrix and guest molecules leads to low loading efficiency and high leakage of biomolecules. We also compared the performance of COF **1** with other porous materials (for example, MOFs and MCM-41).[38–41] Overall, covalent immobilization of biomolecules using COF **1** is superior to all the other tested porous materials (Figure 2).

We conducted various characterizations on biomolecules⊂COF **1** systems, including scanning electron microscopy (SEM), PXRD, confocal laser scanning microscopy (CLSM), FTIR, ^{13}C CP/MAS NMR, and gas sorption. SEM images (Supporting Information, Figure S9) shows that particles of biomolecules⊂COF **1** retained the same filamentous morphology as pristine COF **1**. Furthermore, PXRD patterns revealed that these biomolecule⊂COF **1** complexes possessed the same structure as parent COF **1** (Figure 1), which indicated that COF **1** is a robust platform for post-modification with biomolecules. To confirm the covalent reaction occurred between the biomolecules and COF **1**, two florescence marks, fluorescein amine and 5-carboxylfluorescein, were used to react with COF **1** and lysozyme, respectively, via the same reaction procedure as the formation of biomolecule⊂COF **1**. After the reactions, the samples were thoroughly washed to remove the unreacted florescence marks, and then scanned by CLSM. We observed that florescence marks were uniformly dispersed in both the modified lysozyme and COF **1** samples (Supporting Information, Figure S10), which confirmed the coupling reaction of −NH₂ and −COOH indeed happened. Fluorescein amine labeled lysozyme was also immobilized into COF **1** to determine the distribution of lysozyme in COF **1**, and CLSM results indicated that lysozyme is not just attached on the surface of COF **1**, but uniformly distributed in COF **1** (Figure 3 a–c). Owing to the existence of amide groups in lysozyme and peptide, we selected aminofluorescein⊂COF **1** and lysine⊂COF **1** as representatives to study the formation of covalent bonds (that is, amide) between the framework and biomolecules. The characteristic FTIR peaks at about 1240 and about 3400 cm⁻¹
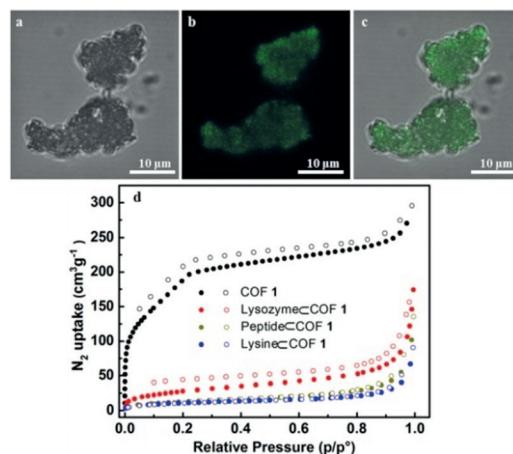

Figure 3. CLSM images of fluorescein-labeled lysozyme covalently immobilized in COF **1**: a) optical image, b) fluorescent, and c) overlap of optical and fluorescent images. d) N₂ sorption isotherms of COF **1** (black), lysozyme⊂COF **1** (red), peptide⊂COF **1** (dark yellow), and lysine⊂COF **1** (blue).

were observed, which can be ascribed to C−N and N−H bond stretching vibrations of amide groups formed by reaction of −COOH and −NH₂ (Supporting Information, Figure S11).[42] ^{13}C CP/MAS NMR spectrum of aminofluorescein⊂COF **1** and lysine⊂COF **1** both showed the characteristic carbonyl carbon peaks of amide at about 170 ppm (Supporting Information, Figure S3). All these results verified the coupling reactions indeed occurred between −NH₂ and −COOH of COF **1**. To further confirm the biomolecules are located inside the channels of COF **1**, we compared COF **1** porosity before and after covalent immobilization. COF **1** possesses a BET and Langmuir surface areas of 714 m² g⁻¹ and 1100 m² g⁻¹, respectively (Figure 3 d; Supporting Information, Figure S12). The nonlocal density functional theory (NLDFT) pore size distribution analysis indicates that COF **1** has a pore size distribution centered at 3.7 nm, which is consistent with the simulated structure with hexagonal channels (3.6 nm). After immobilization of biomolecules, the BET and Langmuir surface areas of Lysozyme⊂COF **1** decreased to 103 m² g⁻¹ and 239 m² g⁻¹, respectively. Based on NLDFT pore size distribution analysis, Lysozyme⊂COF **1** has a pore size centered at about 1.5 nm, which is much smaller than COF **1** owing to the blockage of channels by lysozyme. For peptide⊂COF **1** and lysine⊂COF **1**, we also observed similar trend as lysozyme⊂COF **1** that the surface area and pore size decreased after the immobilization of biomolecules. All these results revealed the efficient covalent immobilization of biomolecules into the channels of COF **1**.

The afforded lysozyme⊂COF **1** maintained more than 90% of enzymatic activity (Supporting Information, Figure S13, Table S1), which validated the designed immobilization strategy presents no influence on biomolecule activity. Furthermore, circular dichroism (CD) spectroscopic analysis indicated no significant structural change of lysozyme after covalent immobilization into COF **1** (Supporting Information, Figure S14, Table S2).[43] We further tested the stability and recyclability of lysozyme⊂COF **1** under various treatments including heating, sonication, and various solvent

16756 www.angewandte.org

© 2018 Wiley-VCH Verlag GmbH & Co. KGaA, Weinheim

Angew. Chem. Int. Ed. **2018**, *57*, 16754–16759

treatments (Supporting Information, Figures S15, S16). The results unveiled excellent stability of lysozyme⊂COF **1** (> 85% of activity) after all the treatments, while the free lysozymes nearly lost all the activities after the same treatments. In the reusability test, lysozyme⊂COF **1** retained more than 90% of activity after five catalytic cycles of chitosan hydrolysis (Supporting Information, Figure S17). In contrast, lysozyme@COF **1** prepared by the adsorption method completely lost its activity after five catalytic cycles because of the severe leaching of lysozyme (Supporting Information, Figure S17). The excellent loading and non-leaching performance, together with the high porosity and extraordinary stability of COF **1**, make them good candidates for the preparation of highly efficient and durable CSPs.

The afforded biomolecule⊂COF **1** materials were anticipated to inherit the intrinsic chirality from biomolecules, which will facilitate chiral separation. Thereby, the formed biomolecule⊂COF **1** were employed as biomolecule-based CSPs for chiral separation (Figure 4). They were examined by

Figure 4. a) Illustration of lysozyme⊂COF **1** based CSPs for chiral separation; b)–g) Enantiomer separation chromatograms of b) DL-threonine, c) DL-leucine, d) DL-tryptophan, e) Ofloxacin, f) Metoprolol, and g) chlorpheniramine.

HPLC towards various racemates including DL-tryptophan, DL-leucine, DL-threonine, DL-lysine, DL-aspartic acid, ofloxacin, (+/−)-propranolol hydrochloride, metoprolol tartrate, alanyl glutamine, chlorpheniramine, and benzoin (Supporting Information, Figure S18). The separation factors (α) and resolution (Rs) results demonstrate Lysozyme⊂COF **1** exhibits high chiral separation efficiency for all the tested racemates (Figure 4; Supporting Information, Figures S19–S21 and Table S3). The elution order of the racemates was confirmed through testing pure enantiomer (Supporting Information, Figure S21). It is notable that the dimensions of all the tested racemates are smaller than the pore size of Lysozyme⊂COF **1** (15 Å), implying the chiral separation occurred inside the pores of Lysozyme⊂COF **1**. Moreover, we observed broader and overlapping peaks, and tailing in the

HPLC chromatograms of lysozyme@COF **1** (Supporting Information, Figure S22), which indicated its lower separation efficiency compared to lysozyme⊂COF **1**. This difference is probably due to a lower loading amount and severe leaching of lysozyme in lysozyme@COF **1**, implying the correlation between loading amount of lysozyme and separation efficiency of the formed CSPs. As for lysozyme@MCM-41, even though MCM-41 can load a small amount of lysozyme, the protein was completely leached out even before the baseline was stable in the HPLC test, and thus showed no separation effect (Supporting Information, Figure S23). Furthermore, blank COF **1** and MCM-41 exhibited no separation effect on any of the tested racemates (Supporting Information, Table S4). These results indicate the strategy to covalently immobilize biomolecules into porous matrix surpasses the traditional adsorption immobilization strategy toward chiral separation performance.

The influences of different biomolecules on the chiral separation performance of biomolecules⊂COF **1** was also studied. The separation performance of peptide⊂COF **1** and lysine⊂COF **1** were tested under the same conditions as the lysozyme⊂COF **1** column (Supporting Information, Figures S24, S28). The peptide⊂COF **1** only exhibited separation effect towards some of the tested racemates with low separation efficiency (Supporting Information, Figures S24, S25). This is probably due to the structural simplicity of the peptide (NH_2-Lys-Val-Phe-COOH), which is supported by CD spectroscopic analysis: the structure of the selected peptide was mainly sheet, turn, and unordered structures (37%, 21.6%, and 29.4%, respectively; Supporting Information, Figure S26, S27). Lysine⊂COF **1** failed to separate any of the tested racemates (Supporting Information, Figure S28), which highlighted the importance of higher order structure of biomolecules (for example, lysozyme) in chiral recognition and resolution. It is likely that the resolution abilities of biomolecule⊂COFs are related to the secondary or higher order structures and the number of chiral centers.[11,44] Therefore, surface-enhanced Raman scattering (SERS) spectra were collected to probe the specific interactions between racemic substrates and lysozyme (tryptophan was selected as a representative substrate).[45,46] Compared with lysozyme, Raman spectra of lysozyme mixed with L-tryptophan exhibited the absence of the amide I band at 1651 cm^{-1}, which is assigned to the random coil structure of lysozyme (Supporting Information, Figure S29a). Moreover, the amide I band at 1623 cm^{-1} assigned to α-helical structure and amide III band at 1241 cm^{-1} assigned to random coil structure of lysozyme were blue-shifted to 1596 and 1231 cm^{-1}, respectively. By contrast, after mixing lysozyme with D-tryptophan, we only observed the absence of amide I band at 1651 cm^{-1} assigned to the random coil structure, without observation of any band shift (Supporting Information, Figure S29a). These results indicated that the interaction between the secondary structure of lysozyme and L-tryptophan is more profound than that of D-tryptophan; the HPLC results can be interpreted as that the L-tryptophan was eluted later than the D-enantiomer. In contrast, after mixing with tryptophan, the Raman spectra of the peptide presented no change (Supporting Information, Figure S29b), implying no interaction between peptide and
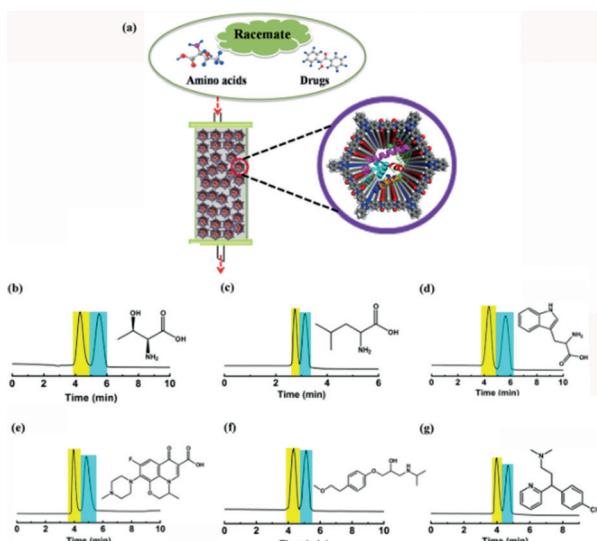
the racemates possibly owing to the lack of secondary structure. These results highlighted that the resolution abilities of biomolecules are related to their secondary or higher order structures.

The interaction between lysozyme and enantiomers mainly manifests as hydrophobic and electrostatic interactions.[47] Due to the amphipathicity of the protein, and the excellent solvent stability of COF **1**, lysozyme⊂COF **1** can act as versatile CSPs for both reverse and normal phase HPLC tests (Supporting Information, Figures S19, S20) with high efficiency, which results in its ability to separate a large range of chiral compounds. Furthermore, lysozyme is covalently immobilized and protected by COF **1**, which leads to good reusability and extended service life (Supporting Information, Table S5). Lysozyme⊂COF **1** CSP demonstrated high efficiency for >120 separation runs during the tested period (2 months) (Supporting Information, Figure S30). Such excellent performance of lysozyme⊂COF **1** entitled its great potential to serve as a versatile and durable protein-based CSP.

In summary, we demonstrated for the first time the successful anchoring of a series of biomolecules (lysozyme, tripeptide, and L-lysine) into a newly synthesized polyimide achiral COF (biomolecule⊂COF **1**) through covalent immobilization to enrich chirality of COF. Inheriting the strong chirality and specific interactions from the anchored biomolecules, the afforded lysozyme⊂COF **1** exhibited versatile and high chiral separation efficiency for various racemates in both normal-phase and reverse-phase HPLC, and demonstrated good reusability and reproducibility due to the protection of COFs. Surface-enhanced Raman scattering studies unveiled that the different interactions between lysozyme secondary structure and racemates account for the observed chiral separation capacity. Furthermore, by evaluating the chiral separation capacities of biomolecule⊂COF **1**, we discovered that the resolution abilities are likely related to the structural complexity, number of chiral centers, and amphipathicity of biomolecules. This study will promote the wide applications of COFs in chiral separation and provide valuable guidance on design of highly efficient and durable biomolecule-based CSPs.

Conflict of interest

The authors declare no conflict of interest.

[1] K. Neeraj, S. Upendra, S. Chitra, S. Bikram, *Curr. Top. Med. Chem.* **2012**, *12*, 1436–1455.
[2] S. M. Xie, L. M. Yuan, *J. Sep. Sci.* **2017**, *40*, 124–137.
[3] S. Y. Zhang, C. X. Yang, W. Shi, X. P. Yan, P. Cheng, L. Wojtas, M. J. Zaworotko, *Chem* **2017**, *3*, 281–289.
[4] S. Das, S. Xu, T. Ben, S. Qiu, *Angew. Chem. Int. Ed.* **2018**, *57*, 8629–8633; *Angew. Chem.* **2018**, *130*, 8765–8769.
[5] T. Jacobs, R. Clowes, A. I. Cooper, M. J. Hardie, *Angew. Chem. Int. Ed.* **2012**, *51*, 5192–5195; *Angew. Chem.* **2012**, *124*, 5282–5285.
[6] Q. Han, B. Qi, W. Ren, C. He, J. Niu, C. Duan, *Nat. Commun.* **2015**, *6*, 10007.
[7] J. Shen, Y. Okamato, *Chem. Rev.* **2016**, *116*, 1094–1138.
[8] P. Levkin, N. M. Maier, W. Lindner, V. Schurig, *J. Chromatogr. A* **2012**, *1269*, 270–278.
[9] A. Berthod, W. Li, D. W. Armstrong, *Anal. Chem.* **1992**, *64*, 873–879.
[10] A. Cavazzini, G. Nadalini, F. Dondi, F. Gasparrini, *J. Chromatogr. A* **2004**, *1031*, 143–158.
[11] C. Bi, X. Zheng, S. Azaria, S. Beeram, Z. Li, D. S. Hage, *Separations* **2016**, *3*, 27.
[12] Y. Song, Q. Sun, B. Aguila, S. Ma, *Adv. Sci.* **2018**, https://doi.org/10.1002/advs.201801410.
[13] C. Qian, Q. Y. Qi, G. F. Jiang, F. Z. Cui, Y. Tian, X. Zhao, *J. Am. Chem. Soc.* **2017**, *139*, 6736–6743.
[14] N. Huang, P. Wang, D. Jiang, *Nat. Rev. Mater.* **2016**, *1*, 16068.
[15] H. Furukawa, O. M. Yaghi, *J. Am. Chem. Soc.* **2009**, *131*, 8875–8883.
[16] E. Jin, M. Asada, Q. Xu, S. Dalapati, M. A. Addicoat, M. A. Brady, H. Xu, T. Nakamura, T. Heine, Q. Chen, D. Jiang, *Science* **2017**, *357*, 673–676.
[17] H. S. Xu, S. Y. Ding, W. K. An, H. Wu, W. Wang, *J. Am. Chem. Soc.* **2016**, *138*, 11489–11492.
[18] X. Han, Q. Xia, J. Huang, Y. Liu, C. Tan, Y. Cui, *J. Am. Chem. Soc.* **2017**, *139*, 8693–8697.
[19] H. Xu, J. Gao, D. Jiang, *Nat. Chem.* **2015**, *7*, 905–912.
[20] Q. Sun, B. Aguila, L. D. Earl, C. W. Abney, L. Wojtas, P. K. Thallapally, S. Ma, *Adv. Mater.* **2018**, *30*, 1705479.
[21] Q. Fang, J. Wang, S. Gu, R. B. Kaspar, Z. Zhuang, J. Zheng, H. Guo, S. Qiu, Y. Yan, *J. Am. Chem. Soc.* **2015**, *137*, 8352–8355.
[22] Q. Sun, B. Aguila, J. Perman, T. Butts, F.-S. Xiao, S. Ma, *Chem* **2018**, *4*, 1726–1739.
[23] H. L. Qian, C. X. Yang, X. P. Yan, *Nat. Commun.* **2016**, *7*, 12104.
[24] X. Han, J. Huang, C. Yuan, Y. Liu, Y. Cui, *J. Am. Chem. Soc.* **2018**, *140*, 892–895.
[25] H. L. Qian, C. X. Yang, W. L. Wang, C. Yang, X. P. Yan, *J. Chromatogr. A* **2018**, *1542*, 1–18.
[26] Q. Sun, C. W. Fu, B. Aguila, J. Perman, S. Wang, H. Y. Huang, F. S. Xiao, S. Ma, *J. Am. Chem. Soc.* **2018**, *140*, 984–992.
[27] G. T. Hermanson, A. K. Mallia, P. K. Smith, *Immobilized affinity ligand techniques*, Academic Press, New York, **1992**.
[28] R. Messing, *Immobilized Enzymes For Industrial Reactors*, Academic Press, New York, **1975**.
[29] H. Weetall, *Immobilized Enzyme Technology: Research and Applications*, Springer Science & Business Media, Cham, **2012**.
[30] C. C. F. Blake, D. F. Koenig, G. A. Mair, A. C. T. North, D. C. Phillips, V. R. Sarma, *Nature* **1965**, *206*, 757–761.
[31] Q. R. Fang, Z. Zhuang, S. Gu, R. B. Kaspar, J. Zheng, J. Wang, S. Qiu, Y. Yan, *Nat. Commun.* **2014**, *5*, 4503.
[32] B. Lu, T. C. Chung, *Macromolecules* **1999**, *32*, 8678–8680.
[33] E. T. Kang, K. L. Tan, *Macromolecules* **1996**, *29*, 6872–6879.

[34] Q. Lu, Y. Ma, H. Li, X. Guan, Y. Yusran, M. Xue, Q. Fang, Y. Yan, S. Qiu, V. Valtchev, *Angew. Chem. Int. Ed.* **2018**, *57*, 6042–6048; *Angew. Chem.* **2018**, *130*, 6150–6156.

[35] S. C. Tsang, Y. K. Chen, P. J. F. Harris, M. L. H. Green, *Nature* **1994**, *372*, 159–162.

[36] D. Samanta, A. Sarkar, *Chem. Soc. Rev.* **2011**, *40*, 2567–2592.

[37] J. S. Kahn, L. Freage, N. Enkin, M. A. A. Garcia, I. Willner, *Adv. Mater.* **2017**, *29*, 1602782.

[38] P. Li, Q. Chen, T. C. Wang, N. A. Vermeulen, B. L. Mehdi, A. Dohnalkova, N. D. Browning, D. Shen, R. Anderson, D. A. Gómez-Gualdrón, F. M. Cetin, J. Jagiello, A. M. Asiri, J. F. Stoddart, O. K. Farha, *Chem* **2018**, *4*, 1022–1034.

[39] V. Lykourinou, Y. Chen, X. S. Wang, L. Meng, T. Hoang, L. J. Ming, R. L. Musselman, S. Ma, *J. Am. Chem. Soc.* **2011**, *133*, 10382–10385.

[40] S. Yuan, J. S. Qin, L. Zou, Y. Chen, X. Wang, Q. Zhang, H. C. Zhou, *J. Am. Chem. Soc.* **2016**, *138*, 6636–6642.

[41] Y. Chen, S. Han, X. Li, Z. Zhang, S. Ma, *Inorg. Chem.* **2014**, *53*, 10006–10008.

[42] J. Gao, B. Zhao, M. E. Itkis, E. Bekyarova, H. Hu, V. Kranak, A. Yu, R. C. Haddon, *J. Am. Chem. Soc.* **2006**, *128*, 7492–7496.

[43] R. Rajan, K. Matsumura, *Sci. Rep.* **2017**, *7*, 45777.

[44] S. Bocian, M. Skoczylas, B. Buszewski, *J. Sep. Sci.* **2016**, *39*, 83–92.

[45] L.-J. Xu, C. Zong, X.-S. Zheng, P. Hu, J.-M. Feng, B. Ren, *Anal. Chem.* **2014**, *86*, 2238–2245.

[46] E. Podstawka, Y. Ozaki, L. M. Proniewicz, *Appl. Spectrosc.* **2004**, *58*, 1147–1156.

[47] Y. Zheng, X. Wang, Y. Ji, *Talanta* **2012**, *91*, 7–17.